A Dynamic Least-Cost Path Method for Incorporating the Street-level Built Environment into Mode Choice Utility

Corin Staves*[1], Qin Zhang[1], Rolf Moeckel[2], Aruna Sivakumar[3], Tayebeh Saghapour[4], Ismail Saadi[1], SM Labib[5], James Woodcock[1], Belen Zapata-Diomedi[4]

[1] MRC Epidemiology Unit, University of Cambridge
[2] Travel Behaviour Modelling, Technical University of Munich
[3] Faculty of Engineering, Imperial College London
[4] Centre for Urban Research, Royal Melbourne Institute of Technology
[5] Faculty of Geosciences, Utrecht University

SHORT SUMMARY

The street-level built environment (BE) describes the micro-environment we experience along paths and streets, such as greenness, slope, walking/cycling infrastructure, and motor vehicle traffic. With greater availability of street-level BE data, there is an emerging body of empirical literature linking street-level BE with mode choice. A common method for developing BE predictors for mode choice is to aggregate attributes along estimated routes between the trip origins and destinations. However, the requirement to pre-specify routing parameters has methodological and behavioural inconsistencies that could cause an underestimation of the significance and influence of street-level BE. This study proposes a method in which routing parameters adapt dynamically to the estimated BE predictors during maximum likelihood estimation. With a demonstration for Greater Manchester, we show that this method produces plausible outputs that can more effectively capture the influence of the street-level BE on behaviour.

Keywords: Discrete choice modelling, Cycling and walking behaviour and design, Built environment

1. INTRODUCTION

There is a large and growing body of empirical research linking the street-level built environment (BE) with walking and cycling (Owen et al., 2004; Cervero et al., 2019; Cain et al., 2017). For example, dedicated infrastructure and urban greenspace is often positively associated with walking and cycling, while steep gradients are negatively associated with cycling (Grudgings et al., 2023; Lovelace et al., 2017; Lu et al., 2018, 2019). Logistic regression models including mode choice are a common tool for empirically estimating the influence of street-level BE on active travel.

When incorporating BE into mode choice, most studies use location-based predictors which describe the area around the trip origin, destination, and/or household. These are simple to develop but vulnerable to the modifiable aerial unit problem, with their size and scale influencing modelled relationships (Strominger et al., 2016; Labib et al., 2020). They do not capture BE along the journey between the origin and destination, which is an important component in decision-making.

Route-based predictors describe the street-level BE along estimated routes between origins and destinations. They evaluate BE as an indicator of impedance, consistent with the way perceptions of impedance are captured for other modes (e.g., cost and waiting time for public transport). However, a key methodological limitation is the assumption about which route to evaluate. Most studies evaluate the shortest or fastest path (Rodríguez & Joo, 2004; Winters et al., 2010; Grudgings et al., 2023). However, this could be a poor indicator of what is actually available for the trip, particularly since cyclists and pedestrians often deviate from the shortest path to use more suitable infrastructure (Dalton et al., 2015).

Alternatively, one could use 'optimal' paths based on a route choice model, as in Broach and Dill (2016). This offers a more empirical basis but chosen route data has limitations regarding data availability and selection bias. In Broach and Dill's results, the estimated BE coefficients from their mode choice model differed substantially from the BE coefficients used to prepare 'optimal' paths. This reveals a crucial methodological limitation: fixed-route BE predictors require assuming sensitivities to the street-level BE for an analysis which aims to measure those same sensitivities empirically. In other words, the input routing assumption becomes contradicted by the results. Given these limitations, using fixed-route indicators could underestimate the significance and influence of the BE.

To address the limitations of using a single route, several studies defined buffer regions around the shortest route to estimate BE predictors (Badland et al., 2008; Winters et al., 2010; Cole-Hunter et al., 2015; Cervero et al., 2019). These approaches are more likely to capture relevant routes in their predictor, but they also capture many irrelevant routes which adds noise and makes results difficult to interpret. Furthermore, results from buffer-based analyses have proven highly sensitive to the buffer extent (Sarjala, 2019).

This study presents a new methodology for incorporating street-level BE predictors into mode choice utility. We define route-based indicators that eliminate the requirement for fixed assumptions about which route to evaluate. Rather than specifying the routing BE sensitivities beforehand, we assume they should match the BE sensitivities being estimated in the mode choice model. This calls for a dynamic estimation process which incorporates least-cost path (LCP) calculations into maximum likelihood estimation (MLE). With each iteration of the MLE, new routing parameters are taken from the current mode choice coefficients and used to recalculate the LCP and corresponding cost for each diary record. This paper examines the feasibility of this dynamic approach regarding convergence of the non-differentiable MLE, interpretation of empirical results, computational considerations, and differences versus fixed-route methods.

2. STUDY AREA

We test our methodology for Greater Manchester in north-west England. We use travel diary data from their local authority, Transport for Greater Manchester (TfGM), containing 7576 commute trips and 13536 discretionary trips.

A multimodal transport network enriched with link (i.e., street segment) level BE attributes was developed from multiple sources using the methodology in Labib et al (2022). We include four link-level BE attributes in this study, which are described in table 1 with example maps in figure 1. These attributes are continuous and defined such that lower values indicate better conditions.

Table 1: Link-level BE attributes

Street-level attribute	**Description**	**Lower bound**	**Upper bound**
Gradient	Elevation increase divided by link length (meters / meters)	0 (flat or downhill)	0.5 (slope ≥ 45º)
Greenness	Viewshed greenness visibility index (VGVI) at eye level. Modelled using data on terrain, surface, land use, and land cover. Further details in Labib et al (2021).	0 (high green visibility with VGVI ≥ 0.9)	1 (no green visibility with VGVI = 0)
Link stress	Discomfort associated with travelling alongside motor vehicles. Modelled using data on pedestrian/cycle infrastructure, speed limits, observed speeds, traffic volumes, and heavy vehicle infrastructure. Further details in Staves et al. (2023)	0 (low stress, e.g., offroad paths, quiet roads)	1 (high stress, e.g., faster and/or busier roads with no dedicated infrastructure)
Junction stress	Discomfort associated with crossing motor vehicles at junctions. Modelled using data on pedestrian/cycle/car signals, speed limits, observed speeds, junction widths and traffic volumes. Further details in Staves et al. (2023)	0 (low stress, e.g., crossing slower roads with dedicated pedestrian/cycle signals)	1 (high stress, e.g., crossing fast or busy junctions without signals)

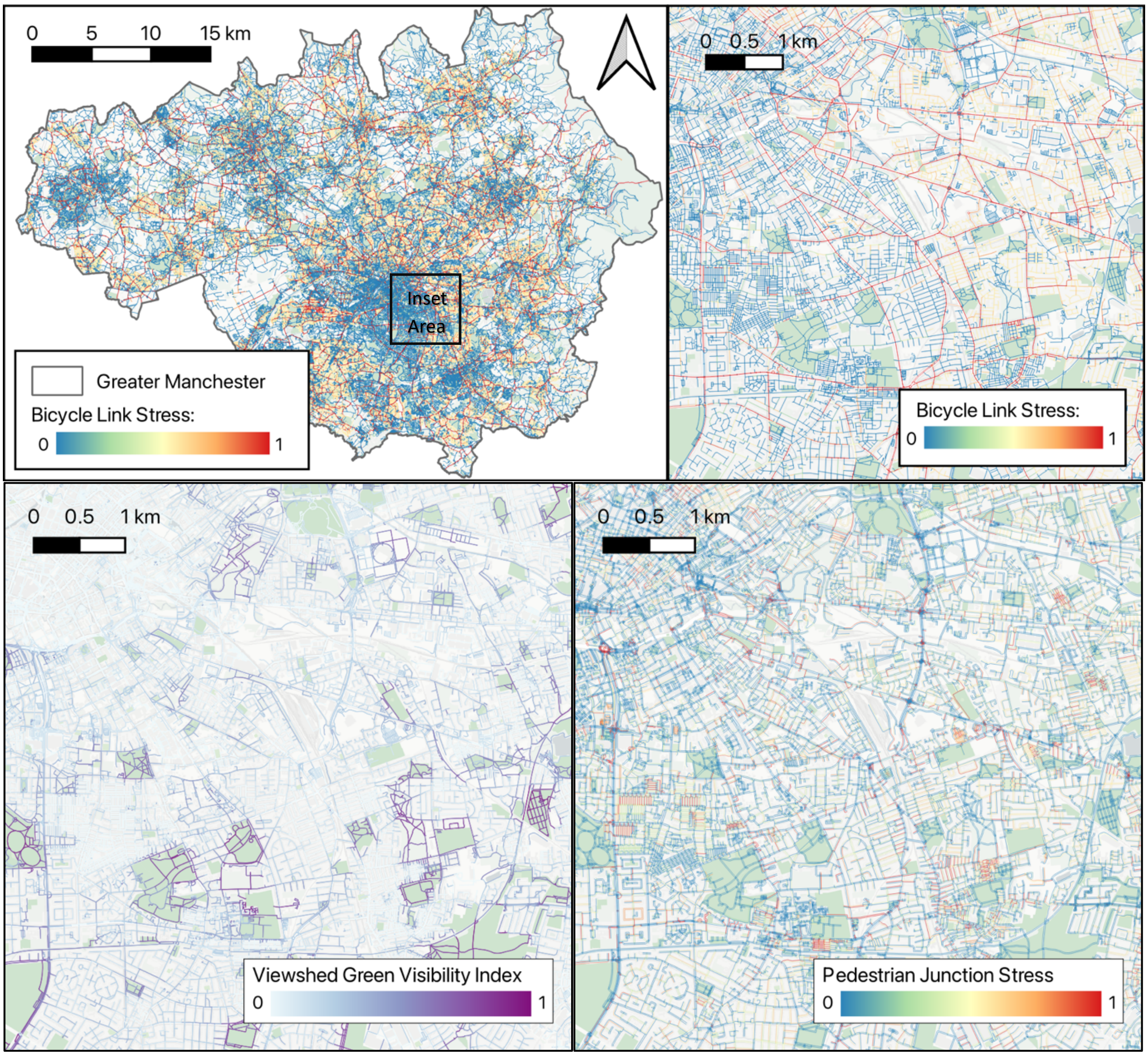

FIGURE 1: Examples of link-level BE attributes for Greater Manchester including bicycle link stress, viewshed green visibility index, and pedestrian junction stress (defined by the stress of junction at the end of each link).

3. METHODOLOGY

Cost

For each mode we define a function of impedance, or cost c_l, for each link l on the network

$$c_l = t_l(1 + \boldsymbol{\gamma}\boldsymbol{a_l}) \tag{1}$$

Where t_l is travel time, $\boldsymbol{a_l}$ is a vector of link-level BE attributes for walking and cycling ($\boldsymbol{a_l} = \mathbf{0}$ for other modes), and $\boldsymbol{\gamma}$ is the corresponding vector of coefficients describing the equivalent travel time penalty for a marginal increase in $\boldsymbol{a_l}$. The total cost c_r of a route r is the sum of individual link costs:

$$c_r = \sum_{l \in r} c_l = \sum_{l \in r} t_l(1 + \boldsymbol{\gamma}\boldsymbol{a_l}) \tag{2}$$

Mode Choice Utility

We specify multinomial logit mode choice models for commute and discretionary trips.
Utility $V_{n,ij}$ for trip n from origin i to destination j is defined as

$$V_{n,ij} = \boldsymbol{\beta_b}\boldsymbol{b_n} + \beta_c L(\boldsymbol{\gamma})_{ij} \tag{3}$$

Where $\boldsymbol{b_n}$ is a vector of person, household, and trip attributes, $\boldsymbol{\beta_b}$ is the corresponding vector of coefficients, β_c is the cost coefficient, and $L(\boldsymbol{\gamma})_{ij}$ is the cost c_r of the LCP between i and j. We use MLE to estimate $\boldsymbol{\beta_a}$ and β_c for all modes and $\boldsymbol{\gamma}$ for the active modes. Since $\boldsymbol{\gamma}$ is within the LCP function $L(\boldsymbol{\gamma})_{ij}$, this function must be integrated into the MLE process.

Properties of the LCP Function

A conceptual illustration of the relationship between $L(\boldsymbol{\gamma})$ and $\boldsymbol{\gamma}$ is presented in figure 2. For simplicity, this example shows one dimension of BE and three single-link paths. As shown in the graph, any of these paths could be the LCP depending on the decision-maker's sensitivity γ to the BE attribute a_l. As γ increases, the decision-maker becomes more willing to accept longer travel times for higher-quality BE.

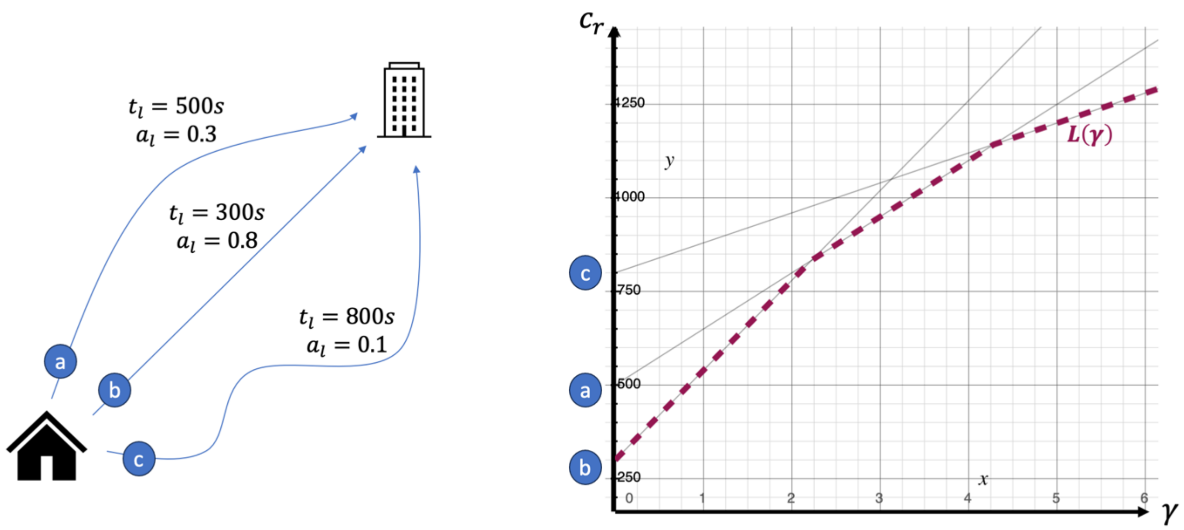

FIGURE 2: Conceptual illustration showing the relationship between $L(\gamma)$ and γ.

The LCP function $L(\gamma)$ is shown as a purple dashed line in figure 2. It has several properties with implications for mode choice utility and MLE. It is continuous and non-linear but made up of linear segments. The slope of $L(\gamma)$ is always positive and remains constant or decreases as γ increases. However, it is non-differentiable with respect to γ, making it impossible to compute analytical gradients during MLE. Generalising to multiple dimensions, $L(\boldsymbol{\gamma})$ becomes a continuous nondifferentiable hypersurface made up of many hyperplanes, each representing a plausible route. The gradient of the hypersurface is highest at the origin and may reduce as any dimension of γ increases.

Approximating the LCP function for MLE

Existing MLE choice modelling packages cannot incorporate an LCP search. We therefore pre-calculate approximations for $L(\boldsymbol{\gamma})$ which are coded into the MLE via a custom function. For each trip record, an approximated hypersurface $\tilde{L}(\boldsymbol{\gamma})$ is calculated using the following process:

1. Define an empty hypersurface $\tilde{L}(\boldsymbol{\gamma}) := \infty \ \forall \boldsymbol{\gamma}$,
2. Define constraints for $\boldsymbol{\gamma}$,
3. Randomly sample values of $\boldsymbol{\gamma}$ within the constraints,
4. For each sample:
    a. Use the Dijkstra algorithm to estimate the LCP based on equation 1,
    b. Compute the cost of the LCP and its partial derivatives with respect to γ. This defines the hyperplane $h(\boldsymbol{\gamma})$ associated with this route.
    c. Redefine $\tilde{L}(\boldsymbol{\gamma}) := \min\left(\tilde{L}(\boldsymbol{\gamma}), h(\boldsymbol{\gamma})\right) \ \forall \boldsymbol{\gamma}$

The approximated hypersurface is only valid within the prespecified constraints for $\boldsymbol{\gamma}$. If the MLE produces estimates for $\boldsymbol{\gamma}$ outside this range, it would be necessary to either constrain the MLE optimisation or expand the constraints for $\tilde{L}(\boldsymbol{\gamma})$. The geometric properties of $\tilde{L}(\boldsymbol{\gamma})$ allow for a close approximation (within the specified constraints), given sufficient samples.

This study uses the Dijkstra LCP algorithm from MATSim (Horni et al., 2016), which is compute-optimised to efficiently calculate LCPs for a high volume of inputs.

Model Estimation

The empirical estimation uses the Apollo choice modelling suite in R (Hess & Palma, 2019). The MLE optimisation was run unconstrained using the Broyden–Fletcher–Goldfarb–Shanno algorithm with numerical gradients. Insignificant coefficients (robust $p > 0.1$) were dropped.

Comparison to Fixed Route Method

We compared our results to equivalent fixed-route specifications based on the shortest path. This converts utility into a linear function, with the specifications otherwise kept identical.

4. RESULTS AND DISCUSSION

LCP Function Approximation

For a travel diary with 21112 records total, the computation of $\tilde{L}(\gamma)$ took around 50 seconds per sample on a desktop workstation with an 8-core Intel Xeon 2.6HGz CPU with 64GB RAM. This study calculated 2500 samples for walking and cycling. Beyond this, additional samples led to only a small share of records ($< 1\%$) discovering new LCPs, indicating a close approximation.

Empirical Model Results

Both MLE estimations successfully converged to a global optimum after 68 and 126 iterations respectively. Empirical model results are shown tables 2 and 3. Sociodemographic attributes $\boldsymbol{\beta}_b$ follow expected patterns; for example, males and higher income individuals are more likely to drive and females are less likely to cycle. The BE coefficients $\boldsymbol{\gamma}$ generally reveal high sensitivities to the street-level BE. For cycling, each percent increase in uphill gradient is equivalent to a 63-67% time penalty. Cycling on stressful paths is equivalent to as much as a 630% penalty versus low-stress paths. These results are high but similar to findings in Broach and Dill (2016). For walking, the junction stress coefficient was as high as 14, suggesting individuals are willing to walk up to 14 times the width of a stressful junction for a better (e.g., signalised) alternative. For non-commute trips, walking on links without green visibility incurs up to a 62% time penalty versus the greenest links.

To test the plausibility of results, we computed the trip-level detours required to use the LCP based on estimated $\boldsymbol{\gamma}$. The average detours for cyclists were 19% for commutes and 22% for non-commutes, which is within the typical range observed in cycling route choice studies (Reggiani et al., 2022). However, average detours for pedestrians were only 1% for commutes and 3% for discretionary trips, which is smaller than observed in pedestrian route choice literature (Sevtsuk et al., 2021; Sevtsuk & Kalvo, 2022). Including more pedestrian-relevant BE attributes could help capture more realistic walking detours.

Comparison to Fixed Route Method

We do not show the full fixed-route results but provide a brief comparison. The final log-likelihoods were slightly lower, indicating a poorer model fit compared to the dynamic LCP method. Most coefficients were similar, except $\boldsymbol{\gamma}$ for link and junction stress which became less significant and much smaller (only 20-50% of the values on tables 2 and 3). This suggests it is difficult to capture sensitivity to stress using only the fastest path. This finding is consistent with commentary in Winters et al. (2010) which predicted that using the fastest path likely underestimates the influence of street-level BE.

Table 2: Results for Commute Trips

		Car Driver	Car Passenger	Public Transport	Bike	Walk
$\boldsymbol{\beta}_b$	ASC		-2.25***	-1.39***	-1.59***	1.97***
	Age under 24		1.27***	1.04***	1.18***	1.21***
	Age 55 and up			-0.33*	-0.97***	
	Male		-0.37***	-0.35***	1.21***	
	Low income			0.73***	0.75**	0.98***
	High income		-0.25*	-0.60***	-0.55**	-0.62***
	Education trip		4.22***	3.17***	1.35***	2.50***
β_c	Cost	-0.15***	-0.15***	-0.030***	-0.00085***	-0.0019***
$\boldsymbol{\gamma}$	Gradient ($\Delta m/m$)				66.8***	
	Link stress				6.30***	
	Junction stress					4.27***

Log-likelihood at equal shares: -12166, Final log-likelihood: -6997, Adj. r2: 0.4223
Robust p-value: *** p ≤ 0.001, ** p ≤ 0.01, * p ≤ 0.05, . p ≤ 0.1

Table 3: Results for Non-commute Trips

		Car Driver	Car Passenger	Public Transport	Bike	Walk
$\boldsymbol{\beta}_b$	ASC		-0.17**	-1.67***	-3.71***	2.46***
	Age 5–14		16.08***	14.92***	14.57***	14.41***
	Age 15–24		1.52***	2.24***	1.97***	1.85***
	Age 40–69		-0.20**	0.19.	-0.41*	-0.46***
	Age 70+		0.23**	0.65***	-1.73***	-0.95***
	Male		-1.12***	-0.61***	0.94***	-0.22***
	Low Income			1.17***	1.05***	1.01***
	High Income		-0.30***	-0.49***		
β_c	Cost	-0.21***	-0.21***	-0.051***	-0.00092***	-0.0016***
$\boldsymbol{\gamma}$	Gradient ($\Delta m/m$)				63.45***	
	Greeness					0.62**
	Link stress				1.59***	
	Junction stress					14.34***

Log-likelihood at equal shares: -21774, Final log-likelihood: -12952, Adj. r2: 0.403
Robust p-value: *** p ≤ 0.001, ** p ≤ 0.01, * p ≤ 0.05, . p ≤ 0.1

5. CONCLUSIONS

This paper demonstrates the feasibility of incorporating dynamic LCP functions into mode choice utility to assess the influence of street-level BE. Despite introducing non-linearity and non-differentiability into MLE, the proposed method successfully converges and produces plausible empirical results with higher BE sensitivities than fixed-route methods.

The model specifications and results serve as a proof of concept rather than an informative empirical analysis. Our focus is on the integration of a dynamic LCP function into mode choice utility, so this demonstration applied a simple MNL model framework with a limited number of predictors. We recognise many limitations associated with this specification including the i.i.d. assumption meaning it cannot account for correlated alternatives and/or observations, the lack of key sociodemographic predictors such as car ownership, and the assumption of homogenous tastes toward street-level BE. To address these shortcomings, a more advanced empirical analysis could expand this methodology using additional predictors, nesting structures, interaction variables, random parameters and/or latent classes.

The need to approximate $\tilde{L}(\boldsymbol{\gamma})$ is a limitation. It requires pre-specifying constraints for $\boldsymbol{\gamma}$ that would need to be re-defined if MLE results exceed them. This could prove time-consuming for the analyst, who may have to iterate several times between approximating $\tilde{L}(\boldsymbol{\gamma})$ and testing model specifications. The approximation is computationally expensive, particularly if the sampling space and dimensionality are high. In addition, the approximation requires impedance c_l to be specified as a linear combination of $\boldsymbol{a_l}$ and $\boldsymbol{\gamma}$ (see equation 1). Examining more advanced relationships between the BE and impedance would require adapting this methodology likely reducing the quality of the approximation.

The approximation could be eliminated entirely by integrating an efficient LCP algorithm directly into the MLE algorithm. There would be no need to specify constraints or pre-calculate $\tilde{L}(\boldsymbol{\gamma})$, and c_l could be specified as any function of $\boldsymbol{\gamma}$ provided $c_l > 0$. It would also substantially reduce computational demand: instead of needing enough samples to closely approximate $\tilde{L}(\boldsymbol{\gamma})$ over a range of $\boldsymbol{\gamma}$, routes would only need to be calculated once per MLE iteration. However, achieving an efficient 'tighter' integration would be a considerable programming effort requiring low-level integration of LCP and MLE algorithms.

Designing urban environments to facilitate walking and cycling is increasingly prioritised by planners, modellers, and decision makers. Advances in geospatial science are enabling more widespread and detailed collection of street-level BE data, providing increasing opportunities to incorporate BE into empirical work and simulations. The dynamic method proposed in this study has considerable potential to advance the way we model the impacts of street-level BE on travel behaviour and can help modellers to more effectively capture its influence on active travel decisions.

ACKNOWLEDGEMENTS

This study was supported by the UKRI-NHMRC Built Environment Prevention Research Scheme (#MR/T038578/1, APP1192788) and the European Research Council under the Horizon 2020 research and innovation program (grant agreement No 817754). We are grateful to TfGM for their support in providing travel diary and BE data.

REFERENCES

Badland, H. M., Schofield, G. M., & Garrett, N. (2008). Travel behavior and objectively measured urban design variables: Associations for adults traveling to work. *Health & Place*, *14*(1), 85–95. https://doi.org/10.1016/j.healthplace.2007.05.002

Broach, J., & Dill, J. (2016). Using Predicted Bicyclist and Pedestrian Route Choice to Enhance Mode Choice Models. *Transportation Research Record: Journal of the Transportation Research Board*, *2564*(1), 52–59. https://doi.org/10.3141/2564-06

Cain, K. L., Gavand, K. A., Conway, T. L., Geremia, C. M., Millstein, R. A., Frank, L. D., Saelens, B. E., Adams, M. A., Glanz, K., King, A. C., & Sallis, J. F. (2017). Developing and validating an abbreviated version of the Microscale Audit for Pedestrian Streetscapes (MAPS-Abbreviated). *Journal of Transport & Health*, *5*, 84–96. https://doi.org/10.1016/j.jth.2017.05.004

Cervero, R., Denman, S., & Jin, Y. (2019). Network design, built and natural environments, and bicycle commuting: Evidence from British cities and towns. *Transport Policy*, *74*, 153–164. https://doi.org/10.1016/j.tranpol.2018.09.007

Cole-Hunter, T., Donaire-Gonzalez, D., Curto, A., Ambros, A., Valentin, A., Garcia-Aymerich, J., Martínez, D., Braun, L. M., Mendez, M., Jerrett, M., Rodriguez, D., De Nazelle, A., & Nieuwenhuijsen, M. (2015). Objective correlates and determinants of bicycle commuting propensity in an urban environment. *Transportation Research Part D: Transport and Environment*, *40*, 132–143. https://doi.org/10.1016/j.trd.2015.07.004

Dalton, A. M., Jones, A. P., Panter, J., & Ogilvie, D. (2015). Are GIS-modelled routes a useful proxy for the actual routes followed by commuters? *Journal of Transport & Health*, *2*(2), 219–229. https://doi.org/10.1016/j.jth.2014.10.001

Grudgings, N., Hughes, S., & Hagen-Zanker, A. (2023). What aspects of traffic intensity most influence cycling mode choice? A study of commuting in Surrey, UK. *International Journal of Sustainable Transportation*, *17*(2), 136–147. https://doi.org/10.1080/15568318.2021.1999539

Hess, S., & Palma, D. (2019). Apollo: A flexible, powerful and customisable freeware package for choice model estimation and application. *Journal of Choice Modelling*, *32*, 100170. https://doi.org/10.1016/j.jocm.2019.100170

Horni, A., Nagel, K., & Axhausen, K. (Eds.). (2016). *Multi-Agent Transport Simulation MATSim*. Ubiquity Press. https://doi.org/10.5334/baw

Labib, S. M., Huck, J. J., & Lindley, S. (2021). Modelling and mapping eye-level greenness visibility exposure using multi-source data at high spatial resolutions. *Science of The Total Environment*, *755*, 143050. https://doi.org/10.1016/j.scitotenv.2020.143050

Labib, S. M., Itova, I., Staves, C., Zapata-Diomedi, B., Both, A., Gunn, L., Khreis, H., Abbas, A., Sivakumar, A., Panter, J., Giles-Corti, B., & Woodcock, J. (2022, March 28). *Integrating spatially detailed micro-environmental attributes to a routable transport network for active travel modelling: A pilot study in Greater Manchester*. 30th Annual Geographical Information Science Research UK (GISRUK), Liverpool, United Kingdom. https://doi.org/10.5281/zenodo.6411626

Labib, S. M., Lindley, S., & Huck, J. J. (2020). Scale effects in remotely sensed greenspace metrics and how to mitigate them for environmental health exposure assessment. *Computers, Environment and Urban Systems*, *82*, 101501. https://doi.org/10.1016/j.compenvurbsys.2020.101501

Lovelace, R., Goodman, A., Aldred, R., Berkoff, N., Abbas, A., & Woodcock, J. (2017). The Propensity to Cycle Tool: An open source online system for sustainable transport planning. *Journal of Transport and Land Use*, *10*(1 SE-). https://doi.org/10.5198/jtlu.2016.862

Lu, Y., Sarkar, C., & Xiao, Y. (2018). The effect of street-level greenery on walking behavior: Evidence from Hong Kong. *Social Science & Medicine*, *208*, 41–49. https://doi.org/10.1016/j.socscimed.2018.05.022

Lu, Y., Yang, Y., Sun, G., & Gou, Z. (2019). Associations between overhead-view and eye-level urban greenness and cycling behaviors. *Cities*, *88*, 10–18. https://doi.org/10.1016/j.cities.2019.01.003

Owen, N., Humpel, N., Leslie, E., Bauman, A., & Sallis, J. F. (2004). Understanding environmental influences on walking. *American Journal of Preventive Medicine*, *27*(1), 67–76. https://doi.org/10.1016/j.amepre.2004.03.006

Reggiani, G., Van Oijen, T., Hamedmoghadam, H., Daamen, W., Vu, H. L., & Hoogendoorn, S. (2022). Understanding bikeability: A methodology to assess urban networks. *Transportation*, *49*(3), 897–925. https://doi.org/10.1007/s11116-021-10198-0

Rodríguez, D. A., & Joo, J. (2004). The relationship between non-motorized mode choice and the local physical environment. *Transportation Research Part D: Transport and Environment*, *9*(2), 151–173. https://doi.org/10.1016/j.trd.2003.11.001

Sarjala, S. (2019). Built environment determinants of pedestrians′ and bicyclists′ route choices on commute trips: Applying a new grid-based method for measuring the built environment along the route. *Journal of Transport Geography*, *78*, 56–69. https://doi.org/10.1016/j.jtrangeo.2019.05.004

Sevtsuk, A., Basu, R., Li, X., & Kalvo, R. (2021). A big data approach to understanding pedestrian route choice preferences: Evidence from San Francisco. *Travel Behaviour and Society*, *25*, 41–51. https://doi.org/10.1016/j.tbs.2021.05.010

Sevtsuk, A., & Kalvo, R. (2022). Predicting pedestrian flow along city streets: A comparison of route choice estimation approaches in downtown San Francisco. *International Journal of Sustainable Transportation*, *16*(3), 222–236. https://doi.org/10.1080/15568318.2020.1858377

Staves, C., Labib, S., Itova, I., Zhang, Q., Woodcock, J., Moeckel, R., & Zapata-Diomedi, B. (2023, September 5). *A MATSim-based framework to Incorporate High Resolution Built Environment Data for Modelling Walkability and Cyclability*. MATSim User′s Meeting, Zurich, Switzerland. https://www.ivt.ethz.ch/en/info/news/2023/09/matsim-user-meeting.html

Strominger, J., Anthopolos, R., & Miranda, M. L. (2016). Implications of construction method and spatial scale on measures of the built environment. *International Journal of Health Geographics*, *15*(1), 15. https://doi.org/10.1186/s12942-016-0044-x

Winters, M., Brauer, M., Setton, E. M., & Teschke, K. (2010). Built Environment Influences on Healthy Transportation Choices: Bicycling versus Driving. *Journal of Urban Health*, *87*(6), 969–993. https://doi.org/10.1007/s11524-010-9509-6